Supplementary Information (SI) for Journal of Materials Chemistry C.
This journal is © The Royal Society of Chemistry 2026

Supporting Information

Enhanced Functional Properties of ABC-type Atomic Layer Deposited Ru Thin Films for Advanced Cu Alternative Nanoscale Interconnects

Jeongha Kim,[a] *Debananda Mohapatra,* [a,b] *Yeseul Son,* [a] *Jae Min Jang,* [c] *Sang Bok Kim,* [a] *Tae Eun Hong,* [d] *Taehoon Cheon,* [e] *Bonggeun Shong,* [f] *and Soo-Hyun Kim* [a,b]*

[a] Graduate School of Semiconductor Materials and Devices Engineering, Ulsan National Institute of Science and Technology (UNIST), Ulju-gun, Ulsan 44919, Republic of Korea

[b] Department of Materials Science and Engineering, Ulsan National Institute of Science and Technology (UNIST), Ulju-gun, Ulsan 44919, Republic of Korea

[c] Department of Chemical Engineering, Hongik University, Mapo-gu, Seoul, 04066, Republic of Korea

[d] Korea Basic Science Institute (KBSI) 618-230, Gangseo-gu, Busan 46742, Republic of Korea

[e] Center for Core Research Facilities, Daegu Gyeongbuk Institute of Science & Technology, Sang-ri, Hyeonpung-myeon, Dalseong-gun, Daegu, 711-873, Republic of Korea

[f] Major in Advanced Materials and Semiconductor Engineering, Hanyang University, Ansan-si, Gyeonggi-do 15588, South Korea

E-mail: soohyunsq@unist.ac.kr

Table S1. Comparison of candidate metal materials for semiconductor interconnects in terms of their suitability and properties

Metal	Bulk Resistivity (μΩ·cm)	Electron Mean Free Path (nm)	Figure of Merit (10^{-16} Ω·m^2)	Melting Temperature (°C)	Cost ($/g)	Ref.
Cu	1.7	39.9	6.6	1,085	0.007~0.01	[1]
W	5.3	15.5	8.2	3,380	0.04~0.06	[1]
Mo	5.3	11.2	6.0	2,620	0.015~0.05	[2, 3]
Co	6.2	7.8	4.8	1,495	0.015~0.03	[1, 4]
Ru	7.1	6.6	4.9	2,334	12~16	[1, 5]
Ir	5.2	7.1	3.7	2,446	140~160	[1, 6]
Rh	4.7	6.9	3.2	1,964	150~200	[1, 7]

Metal	Advantages	Limitations
Cu	- Lowest resistivity - Established infrastructure	- Requires diffusion barrier (e.g., TaN) - Poor scaling behavior - Surface & grain boundary scattering issues
W	- Very high melting temperature - High thermal/mechanical stability - Common ALD precursor availability	- High resistivity in ALD form - Poor grain structure without post-treatment - Poor scaling characteristics and the need for a thick barrier layer
Mo	- No need for a barrier layer	- Lack of liquid precursors for metal deposition
Co	- Lower resistivity than Ru - Excellent adhesion to dielectrics - Compatible with Cu/barrier-free schemes	- Susceptible to oxidation - Lower thermal stability than Ru - Easily oxidized
Ru	- Relatively low resistivity among PGM - High thermal stability - High work function (4.7 eV) - ALD feasibility proven	- Poor film adhesion
Ir	- High thermal stability - Low resistivity - Corrosion resistance	- High cost - Thin film synthesis process in the early research stage
Rh	- Stable thin film formation without diffusion barrier - Electromigration resistance - Low resistivity	- High cost - Thin film synthesis process in the early research stage - Only one Rh precursor available compared to other noble metal ALD

Table S2. Comparison of Deposition Characteristics and Thin Film Properties of Various Ru ALD Processes

Precursor	GPC (Å/Cycle)	Incubation Cycles	Deposition Temp. (℃)	Grain size (nm)	Thickness (nm)	Resistivity (μΩ cm)	Ref.
Cyprus	0.5	~50	270	25	25	20	**8**
Rudense	0.83	little	250	~20	~20	~23	**9**
IMBCHDRu	~0.89	11	270	~20	~20	30	**10**
$CpRu(CO)_2Et$	1	45	< 325	~23	~23	~16	**11**
DER	0.4	0	250	10	10	19	**12**
EBCHDRu	1	2	225	20	20	~20	**12**
EBECHRu	0.42	3	225	15	15	24	**14**
$Ru(EtCp)_2$	0.5	~210	300	35	35	15	**15**
$Ru(thd)_3$	0.36	~250	350	NA	NA	<20	**16**
$RuCp_2$	0.45	~250	350	120	120	~13	**17**
EBBDRu	~0.6	15	225	~10	~10	~26	**18**
$Ru(chd)_2$	0.3	~22	300	~5.5	~10	~14	**19**
Carish	0.9	~3	240	10.6	20	16.5	**20**
	1.2	~3	270	11.6	20	16.0	**20**
	1.4	-	300	12.9	20	13.8	**20**
Ru(CpEt)(CpMe)	-	-	-	-	~6.6	26	**21**
Ru(CpEt)(py)	0.5	-	275~350	-	10~15	14~16	**22**
$Ru(DMBD)(CO)_3$	0.67	-	320	-	-	14	**23**
$Ru(TMM)(CO)_3$	1.7	6	220	17.7	~40	12.9	**24**
$Ru(TMM)(CO)_3$	1.1	0	310	24.5	25	13.4	**This study**

*** Cyprus: bis(2,6,6-trimethylcyclohexa-1,3-dienyl)ruthenium**

*** Rudense: (2,4-dimethylpentadienyl)(ethylcyclopentadienyl)ruthenium**

*** IMBCHDRu: isopropylmethylbenzene–cyclohexadiene ruthenium**

*** $CpRu(CO)_2Et$: cyclopentadienylethyl(dicarbonyl)ruthenium**

*** DER: (2,4-dimethylpentadienyl)(ethylcyclopentadienyl)ruthenium**

*** EBCHDRu: ethylbenzene–cyclohexadiene ruthenium**

*** EBECHRu: (ethylbenzyl)(1-ethyl-1,4-cyclohexadienyl)ruthenium**

*** $Ru(EtCp)_2$:bis(ethylcyclopentadienyl)ruthenium**

*** $Ru(thd)_3$: tris(2,2,6,6-tetramethyl-3,5-heptanedionato)ruthenium**

*** $RuCp_2$: bis(cyclopentadienyl)ruthenium**

*** EBBDRu:(ethylbenzene)(1,3-butadiene)ruthenium**

*** $Ru(chd)_2$: bis(η^5-cycloheptadienyl)ruthenium**

*** Carish: dicarbonyl–bis(5-methyl-2,4-hexanedionato)ruthenium**

*** Ru(CpEt)(CpMe): (ethylcyclopentadienyl)(methylcyclopentadienyl)ruthenium**

*** Ru(CpEt)(py): (ethylcyclopentadienyl)(pyrrolyl)ruthenium**

*** $Ru(DMBD)(CO)_3$: tricarbonyl(η^4-2,3-dimethylbutadiene)ruthenium**

*** $Ru(TMM)(CO)_3$: tricarbonyl(trimethylenemethane)ruthenium**

Table S3. Summary of the Properties of Metal or Metallic Thin Films Deposited by ALD, with a Comparison Based on Deposition Temperature

Deposition Material	Precursor	GPC (Å/Cycle)	Resistivity (μΩ·cm)	Thickness (nm)	Deposition Temp. (°C)	Ref.
Ruthenium (Ru)	IMBCHRu	0.86~0.89	~30	~20	270	[25]
		1.36	~40	~20	310	
	$RuCp_2$	1.2	14	~25	300	[26]
		0.45	~20	-	350	[27]
Molybdenum (Mo)	$MoCl_2O_2$	0.22	18.6	24	350	[28]
		0.22	Slight increase	25	450	
Nickel (Ni)	$Ni(acac)_2(tmeda)$	2.1	18.1	-	260	[29]
		~2.6	19.4	-	300	
Iridium (Ir)	TICP	0.41	23.2	15	250	[6]
		~0.50	~27.0	15	300	
TiN	TDMAT	-	~ 500	~ 20	200	[30]

	-	~ 4,700	~175	300

* IMBCHRu: isopropyl-methylbenzene-cyclohexadiene-ruthenium(0)
* $RuCp_2$: bis(cyclopentadienyl)ruthenium(II)
* $Ni(acac)_2$(tmeda): (N,N,N',N'-tetramethylethylenediamine)(bis(2,4-pentanedionato)) nickel(II)
* TICP: tricarbonyl (1,2,3-η)-1,2,3-tri(tert-butyl)-cyclopropenyl iridium
* TDMAT: tetrakis-dimethyl-amino-titanium

Table S4. Comparison of key characteristics, advantages, and limitations of deposition methods

Deposition Method	Reaction	Growth Temperature	Thickness Control	Growth Rate
PVD	Physical adsorption	Low (Room Temp.)	> 50 Å	Fast
CVD	Surface + Vapor phase reaction	High to Middle (600 °C ~ 300 °C)	> 50 Å	Middle
ALD	Surface reaction	Low to Middle (< 500 °C)	> A few Å	Slow
ABC-type ALD	Surface reaction	Low to Middle (< 500 °C)	> A few Å	Slower than ALD

Deposition Method	Advantages	Limitations
PVD	- Low-temperature process - Fast growth - Simple process	- Poor step coverage for high-aspect-ratio structures
CVD	- Good step coverage - Good wafer uniformity	- Requires high temperature - Difficult to control film quality - High risk of contamination
ALD	- Suitable for high-aspect-ratio structures - Excellent uniformity and conformality	- Limited precursor reactivity - Slow growth rate
ABC-type ALD	- Greater flexibility in optimizing process conditions - Improved nucleation and early growth quality - Enhanced film purity and crystallinity	- Increased process complexity - Requires careful precursor selection - Potential for side reactions or losses - Reduced growth rate

Table S5. Comparison of concentrations in 25 nm Thickness AB-type and ABC-type ALD-Ru thin films through SIMS analysis

Process \ Element	C (at.%)	O (at.%)	Ru (at.%)	Total impurities (C+O) (at.%)
AB-type Ru film	0.6	1.0	97.8	1.6
ABC-type Ru film	Less than 0.1	0.3	99.6	0.3

Table S6. Impact of impurity deduction and grain size increase on the electrical performance of ALD thin films

Metal	O impurity (at.%)	C impurity (at.%)	Temperature (°C)	Grain size	Resistivity (μΩ·cm)	Ref.
Ru	< 1.5	< 0.3	300	↓	↑	[1]
	< 0.5	< 0.3	400	↑	↓	
Ru	< SIMS limit	< 2.4	310	↓	~40	[3]
	< SIMS limit	< SIMS limit	270	↑	~30	
Pt	< 0.5	< 0.5	200	↓	17	[31]
	< 0.3	< 0.3	300	↑	13	

Figure S1. The thermally decomposed naked eye looks at a thermally grown SiO_2 substrate at 220 °C, 260 °C, and 310 °C without any reactant gases.

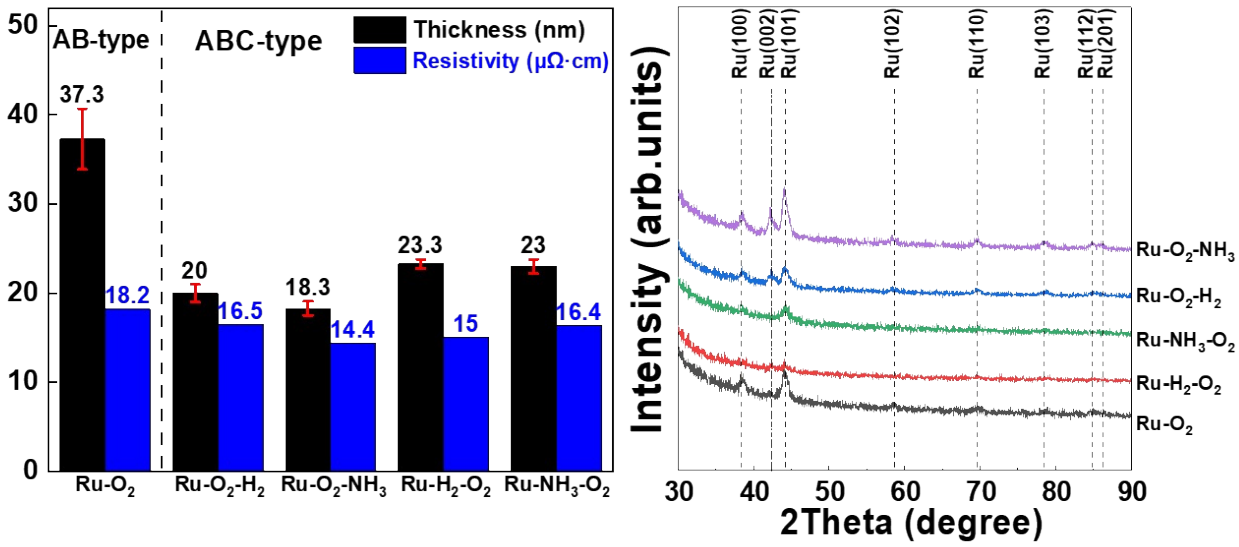

Figure S2. (a) Thickness and resistivity, and (b) XRD patterns of Ru thin films for optimizing the selection of additional reactant gas in the ABC-type Ru ALD experiments.

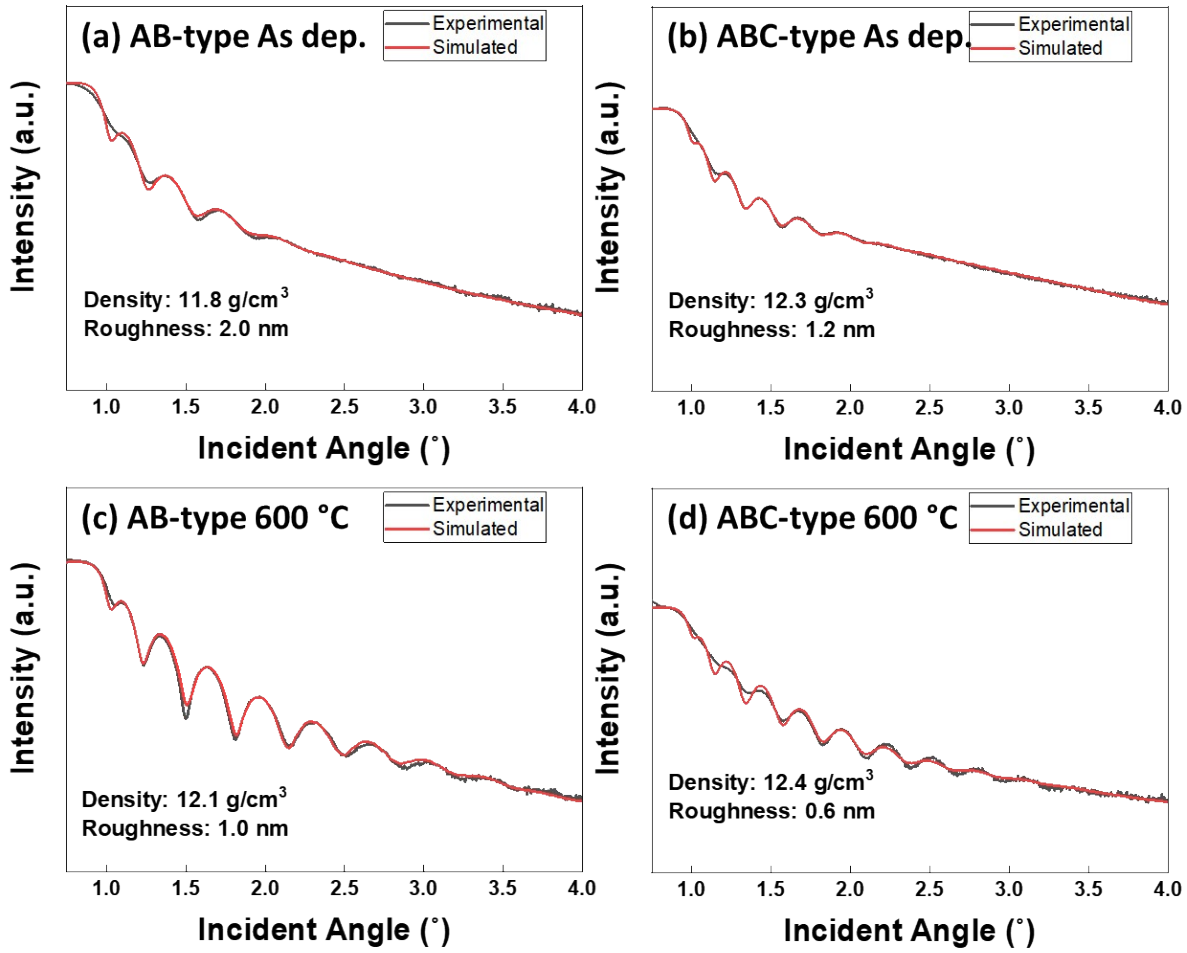

Figure S3. Density and roughness of the films (a) as-deposited AB-type Ru ALD process, (b) as-deposited ABC-type Ru ALD process, (c) AB-type Ru ALD process after 600 °C annealing, and (d) ABC-type Ru ALD process after 600 °C annealing, simulated by X-ray reflectivity (XRR).

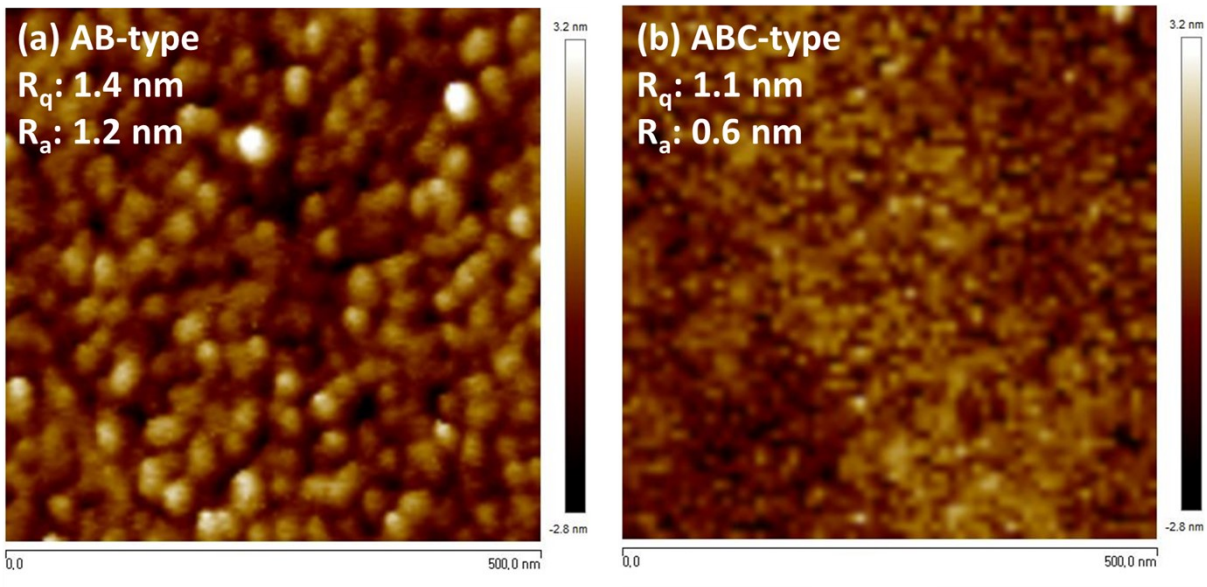

Figure S4. Atomic force microscopy (AFM) surface morphology of Ru thin films deposited by (a) AB-type Ru ALD process and (b) ABC-type Ru ALD process. The surface roughness was measured over a 500 nm × 500 nm area, and the root mean square (R_q) roughness and the average roughness (Ra) were used for evaluation.

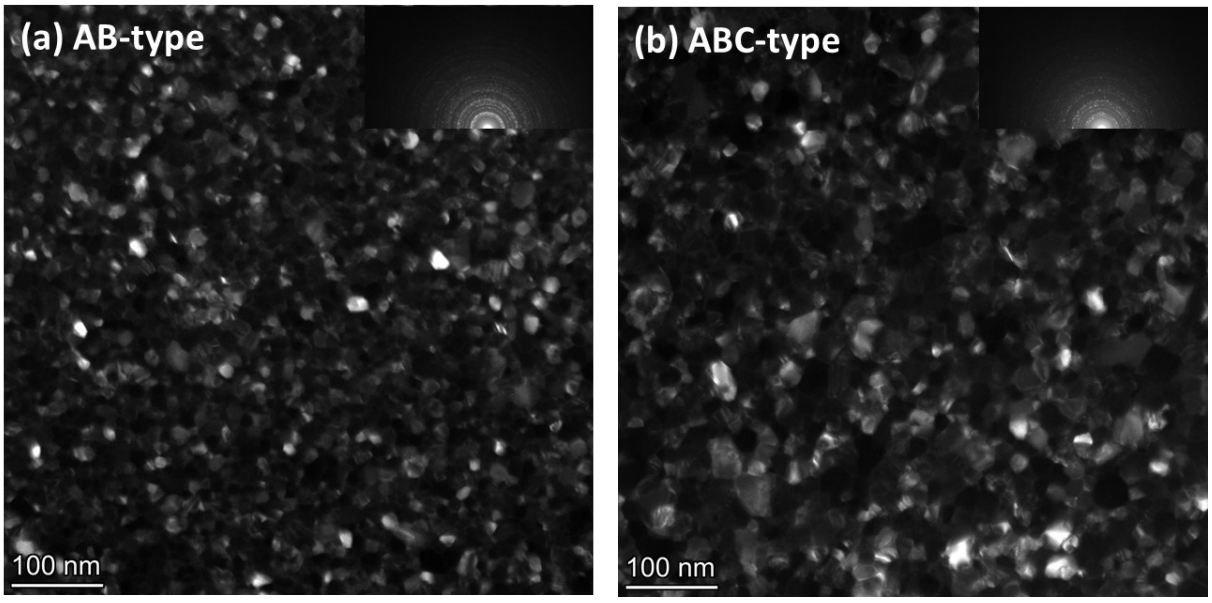

Figure S5. Dark field TEM images of the Ru thin films: (a) AB-type Ru film and (b) ABC-type Ru ALD film.

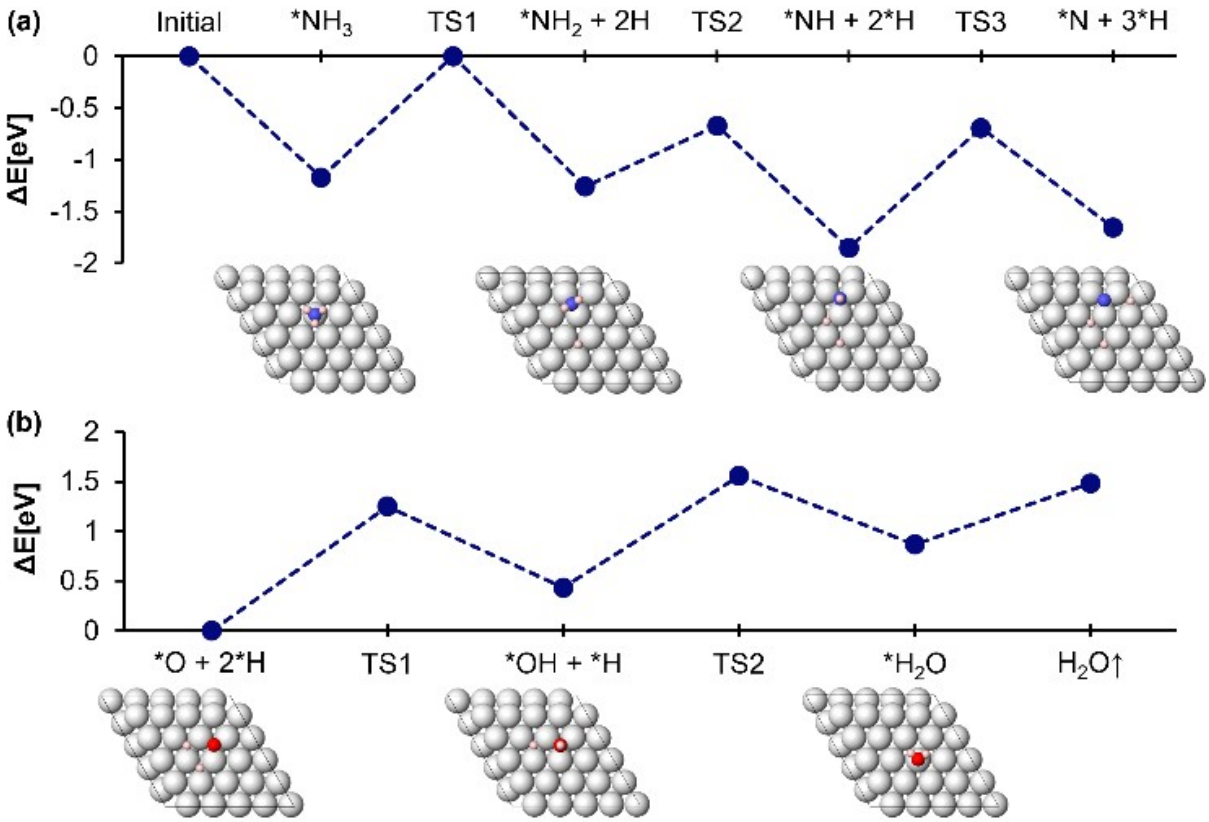

Figure S6. MLP-calculated reaction energy profiles on the Ru (0001) surface. (a) Dissociative adsorption of NH_3 (b) formation of H_2O from H and O adsorbates. Pink = H, blue = N, red = O, and gray = Ru.

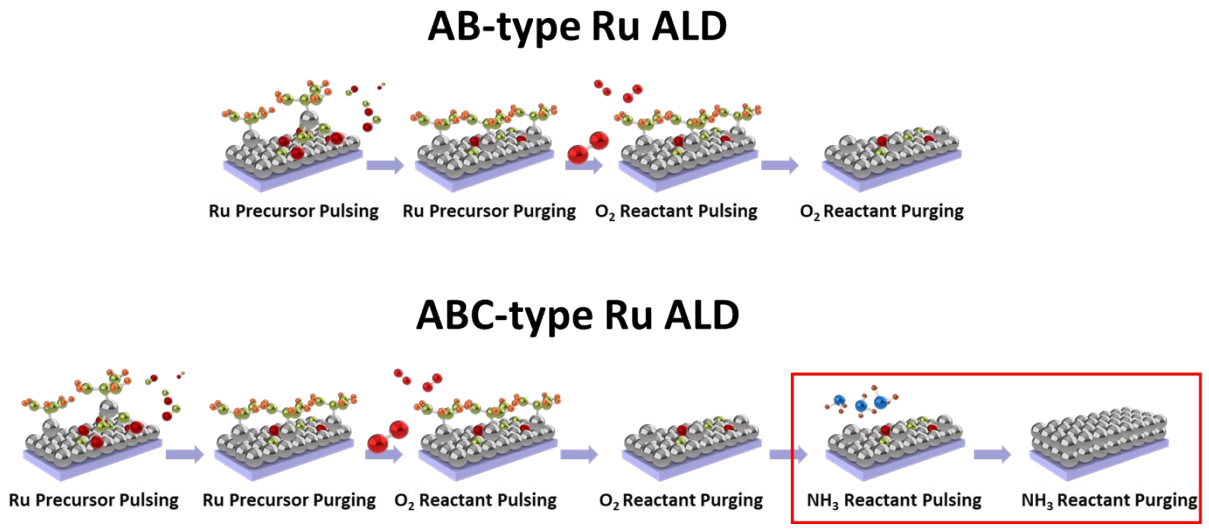

Figure S7. Schematic representation of the AB-type Ru ALD and ABC-type Ru ALD processes to deposit Ru.

Note and Discussion on RBS and SIMS Quantification Interpretations:

The quantification of SIMS data (Figure 2) was performed based on prior Rutherford backscattering spectrometry (RBS) analysis of the same Ru samples. Specifically, the RBS results, which provide an absolute measurement of the elemental composition, were used to establish a calibration factor for each element of interest (C, N, O). This calibration factor was then applied to convert the secondary ion mass spectrometry (SIMS) secondary ion counts into atomic percent (at.%), allowing us to assess impurity concentrations in the Ru thin films quantitatively.

To ensure reliability and reproducibility, we adopted several methodological considerations:

- Depth profiling approach: SIMS measurements were performed across the entire R uthin film thickness, and impurity signals were analyzed only in regions where the Ru signal remained stable. This avoids artifacts from surface contamination or inte rface effects.
- Averaging over a stable region: Instead of using single-point measurements, impuri ty concentrations were calculated by averaging SIMS signals over the composition ally stable region of the film.
- Calibration using RBS: RBS provides atomic concentrations and serves as a reliable standard. By calibrating SIMS signals with RBS data, we can achieve quantitative values even in thin films with nanometer-scale thicknesses.
- Established methodology in literature: The approach of using RBS data to calibrate SIMS is widely recognized and employed in thin film analysis, particularly for m etals and metal oxides, and has been validated in numerous previous studies. Seve ral studies have successfully used this methodology to quantify C, N, O, and othe r impurity levels in Ru and other transition metal thin films.[32-34]

SIMS alone cannot provide absolute quantitative information; however, when combined with RBS-based calibration, it allows for reliable quantitative analysis. In fact, numerous reported cases have demonstrated the successful use of SIMS to perform quantitative analysis of metal thin films deposited by ALD.[35-37] Based on these previous studies, the C, N, and O concentrations in the Ru thin films in this work were obtained using the RBS-calibrated approach, and therefore, the reported quantitative values are considered meaningful and reproducible.

References

[1] D. Gall, *J. Appl. Phys.* **2020**, *127*.

[2] Q. Liu, Q. Huang, *ECS Meet. Abstr.* **2024**, *MA2024-02*, 1891.

[3] B.-J. Lee, K.-B. Lee, M.-H. Cheon, D.-W. Seo, J.-W. Choi, *Coatings* **2023**, *13*, 1070.

[4] M. F. J. Vos, G. Van Straaten, W. M. M. E. Kessels, A. J. M. Mackus, *J. Phys. Chem. C* **2018**, *122*, 22519.

[5] Y. Kotsugi, S.-M. Han, Y.-H. Kim, T. Cheon, D. K. Nandi, R. Ramesh, N.-K. Yu, K. Son, T. Tsugawa, S. Ohtake, R. Harada, Y.-B. Park, B. Shong, S.-H. Kim, *Chem. Mater.* **2021**, *33*, 5639.

[6] N.-Y. Park, M. Kim, Y.-H. Kim, R. Ramesh, D. K. Nandi, T. Tsugawa, T. Shigetomi, K. Suzuki, R. Harada, M. Kim, K.-S. An, B. Shong, S.-H. Kim, *Chem. Mater.* **2022**, *34*, 1533.

[7] Y. Zou, C. Cheng, Y. Guo, A. J. Ong, R. Goei, S. Li, A. I. Y. Tok, *RSC Adv.* **2021**, *11*, 22773.

[8] K. Gregorczyk, L. Henn-Lecordier, J. Gatineau, C. Dussarrat, G. Rubloff, *Chem. Mater.*

2011, 23.

[9] D. S. Kwon, C. H. An, S. H. Kim, D. G. Kim, J. Lim, W. Jeon, C. S. Hwang, *J. Mater. Chem. C* **2020**, 8.

[10] S.-H. Choi, T. Cheon, S.-H. Kim, D.-H. Kang, G.-S. Park, S. Kim, *J. Electrochem. Soc.* **2011**, 158.

[11] N. Leick, R. Verkuijlen, L. Lamagna, E. Langereis, S. Rushworth, F. Roozeboom, M. Van De Sanden, W. Kessels, *J. Vac. Sci. Technol. A* **2011**, 29.

[12] S. K. Kim, S. Y. Lee, S. W. Lee, G. W. Hwang, C. S. Hwang, J. W. Lee, J. Jeong, *J. Electrochem. Soc.* **2007**, 154.

[13] S. Yeo, S.-H. Choi, J.-Y. Park, S.-H. Kim, T. Cheon, B.-Y. Lim, S. Kim, *Thin Solid Films* **2013**, 546.

[14] T. E. Hong, S.-H. Choi, S. Yeo, J.-Y. Park, S.-H. Kim, T. Cheon, H. Kim, M.-K. Kim, H. Kim, ECS *J. Solid State Sci. Technol.* **2012**, 2.

[15] S.-S. Yim, D.-J. Lee, K.-S. Kim, S.-H. Kim, T.-S. Yoon, K.-B. Kim, *J. Appl. Phys.* **2008**, 103.

[16] T. Aaltonen, M. Ritala, K. Arstila, J. Keinonen, M. Leskelä, *Chem. Vap. Depos.* **2004**, 10.

[17] T. Aaltonen, P. Alen, M. Ritala, M. Leskelä, *Chem. Vap. Depos.* **2003**, 9.

[18] S. Yeo, J.-Y. Park, S.-J. Lee, D.-J. Lee, J. H. Seo, S.-H. Kim, *Microelectron. Eng.* **2015**, 137.

[19] J. M. Hwang, S.-M. Han, H. Yang, S. Yeo, S.-H. Lee, C. W. Park, G. H. Kim, B. K. Park, Y. Byun, T. Eom, *J. Mater. Chem. C* **2021**, 9.

[20] E. C. Ko, J. Y. Kim, H. Rhee, K. M. Kim, J. H. Han, *Mater. Sci. Semicond. Process.* **2023**, 156.

[21] K. Kukli, J. Aarik, A. Aidla, T. Uustare, I. Jõgi, J. Lu, M. Tallarida, M. Kemell, A.-A. Kiisler, M. Ritala, *J. Cryst. Growth* **2010**, 312.

[22] K. Kukli, M. Kemell, E. Puukilainen, J. Aarik, A. Aidla, T. Sajavaara, M. Laitinen, M. Tallarida, J. Sundqvist, M. Ritala, *J. Electrochem. Soc.* **2011**, 158.

[23] D. Z. Austin, M. A. Jenkins, D. Allman, S. Hose, D. Price, C. L. Dezelah, J. F. Conley, *Chem. Mater.* **2017**, 29.
[24] S.-H. Kim, N. Kwak, J. Kim, H. Sohn, *J. Electrochem. Soc.* **2006**, 153.
[25] S.-H. Choi, T. Cheon, S.-H. Kim, D.-H. Kang, G.-S. Park, S. Kim, *J. Electrochem. Soc.* **2011**, *158*, D351.

[26] S.-J. Park, W.-H. Kim, H.-B.-R. Lee, W. J. Maeng, H. Kim, *Microelectron. Eng.* **2007**, *85*, 39.

[27] T. Aaltonen, P. Alén, M. Ritala, M. Leskelä, *Chem. Vap. Depos.* **2003**, *9*, 45.

[28] K. Van Der Zouw, B. Y. Van Der Wel, A. a. I. Aarnink, R. a. M. Wolters, D. J. Gravesteijn, A. Y. Kovalgin, *J. Vac. Sci. Technol. A* **2023**, *41*.

[29] Y. Zhang, L. Du, X. Liu, Y. Ding, *Nanoscale* **2018**, *11*, 3484.

[30] H. K. Kim, J. Y. Kim, J. Y. Park, Y. Kim DO, Y. Kim DO, H. T. Jeon, W. M. Kim, *www.osti.gov* **2002**.

[31] T. Aaltonen, M. Ritala, Y.-L. Tung, Y. Chi, K. Arstila, K. Meinander, M. Leskelä, *J. Mater. Res.* **2004**, *19*, 3353.

[32] C. Jeynes, J. L. Colaux, *Analyst.* **2016**, 141(21), 5944-5985.

[33] M. Grasserbauer, *J. Res. Natl. Bur. Stand.* **1988**, 93(3), 510.

[34] C. Jeynes, N. Barradas, E. Szilágyi, *Anal. Chem.* **2012**, 84(14), 6061-6069.

[35] J. Femi-Oyetoro, S. Sypkens, H. LeDuc, M. Dickie, A. Beyer, P. Day, F. Greer, *Appl. Phys. Lett*. **2024**, 125, 6.

[36] M. Popovici, B. Groven, K. Marcoen, Q. M. Phung, S. Dutta, J. Swerts, J. Meersschaut, J. A. van den Berg, A. Franquet, A. Moussa, *Chem. Mater.* **2017**, 29(11), 4654-4666.

[37] S.-J. Lee, S.-H. Kim, M. Saito, K. Suzuki, S. Nabeya, J. Lee, S. Kim, S. Yeom, D.-J. Lee, *J. Vac. Sci. Technol*. *A* **2016**, 34, 3.